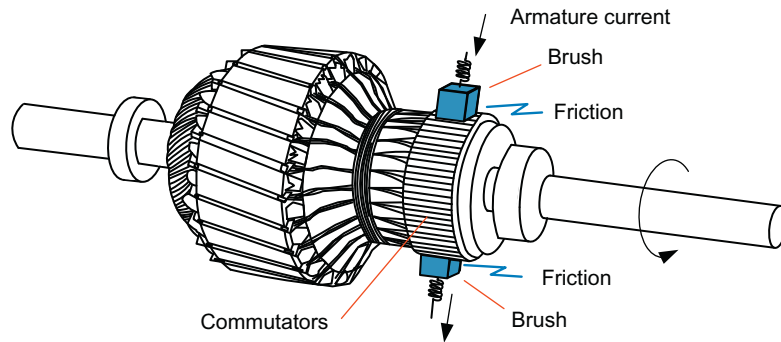# Brushless direct current motors

10

As explained in Chapter 2, direct current (DC) motors need mechanical commutation devices consisting of brushes and commutators that change the direction of the current of conductors to produce an average torque for continuous rotation as shown in Fig. 10.1. However, this mechanical commutation causes an electromagnetic and acoustic noise. The commutators and brushes also need a periodical maintenance and replacement due to wear-out and flashover. Small DC motors with a radius of $\phi25-\phi34$ can operate about 1000 hours, whereas ones with a radius of $\phi37-\phi60$ can operate about 2000 hours. Specially designed DC motors are capable of operating about 3000 hours.

DC motors have been widely used for speed or position control applications because of their control simplicity when compared with alternating current (AC) motors. However, since they require periodic maintenance of brushes and commutators, their utilization has been reduced in many motor drive applications, which require continuous running and enhanced system reliability.

To overcome this problem of DC motors, a motor called *brushless direct current (BLDC) motor* was developed in 1962 [1]. This motor has similar electrical characteristics to a DC motor, but it has an enhanced reliability by replacing mechanical commutation with electronic commutation. To implement the electronic commutation, BLDC motors use sensors and driving circuits. The sensors detect the position of magnets on the rotor. By using the detected magnet position, the driving circuits excite a specific winding for continuous rotation.

In BLDC motors, to eliminate the brushes of DC motors, the armature windings are placed on the stator side and the magnets are placed on the rotor side. As a result, BLDC motors have a different configuration from that of DC motors. Since there is a degree of freedom in the motor configuration when designing to eliminate brushes, various BLDC motor designs to fit a wide application needs such as a smaller or thinner configuration are possible. The BLDC motors have many merits such as high efficiency, high-power density, high torque-to-inertia ratio, high-speed operation capability, simple drive method, and low cost. Thus, nowadays, they are widely used for cost-effective solution in many small and medium motor drive applications such as home appliances, industrial, office products, and light vehicles.

In this chapter, we will discuss the configuration, driving principle, mathematical model, speed and current control, and sensorless techniques of BLDC motors.

FIGURE 10.1

Mechanical commutation devices of a DC motor.
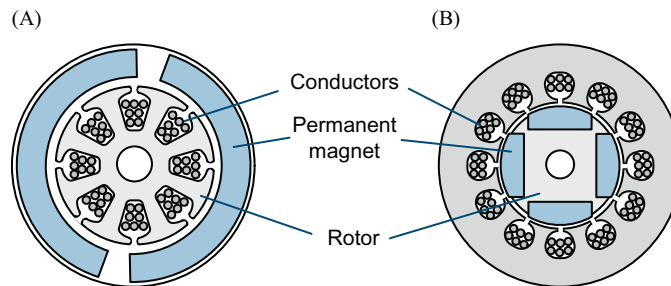
FIGURE 10.2

Configurations of (A) DC motor and (B) BLDC motor.

10.1 CONFIGURATION OF BRUSHLESS DIRECT CURRENT MOTORS

### 10.1.1 COMPARISON BETWEEN BRUSHLESS DIRECT CURRENT MOTORS AND DIRECT CURRENT MOTORS

BLDC motors do not have the crucial weakness of DC motors because the function of brushes and commutators is replaced with semiconductor switches operating based on the information from the rotor position. As a result of this replacement, the configuration of a BLDC motor becomes different from that of a DC motor, but similar to the configuration of a permanent magnet synchronous motor (PMSM). As shown in Fig. 10.2B, the BLDC motor has a configuration in which the windings are placed on the stator side and the magnets on the rotor side. This results in the reversed configuration of a DC motor as shown in Fig. 10.2A. Instead, its configuration resembles that of a PMSM, shown in Fig. 4.8.

However, similar to the current flowing in armature windings of a DC motor, the current flowing in the windings of a BLDC motor is a quasi-square waveform.

Such configuration of BLDC motors has the following merits over DC motors. Compared to the heavy rotor of DC motors consisting of many conductors, BLDC motors have a low inertia rotor. Thus BLDC motors can provide a rapid speed response. Moreover, windings placed on the stator side can easily dissipate heat, allowing BLDC motors to have a better attainable peak torque capability compared to DC motors whose maximum current is limited to avoid the demagnetization of magnets. In addition, BLDC motors can operate at a higher speed because of nonmechanical commutation devices.

10.1.2 COMPARISON BETWEEN BRUSHLESS DIRECT CURRENT MOTORS AND PERMANENT MAGNET SYNCHRONOUS MOTORS

Due to their structural similarity, BLDC motors are often confused with PMSMs. Commonly, BLDC motors can be distinguished from PMSMs by their shape of back-electromotive force (back-EMF). A BLDC motor is designed to develop a trapezoidal back-EMF waveform as shown in Fig. 10.3A. Thus the amplitude of the magnetic flux density generated by the rotor magnets remains constant along the air gap. This can be achieved by using magnets with parallel magnetization.
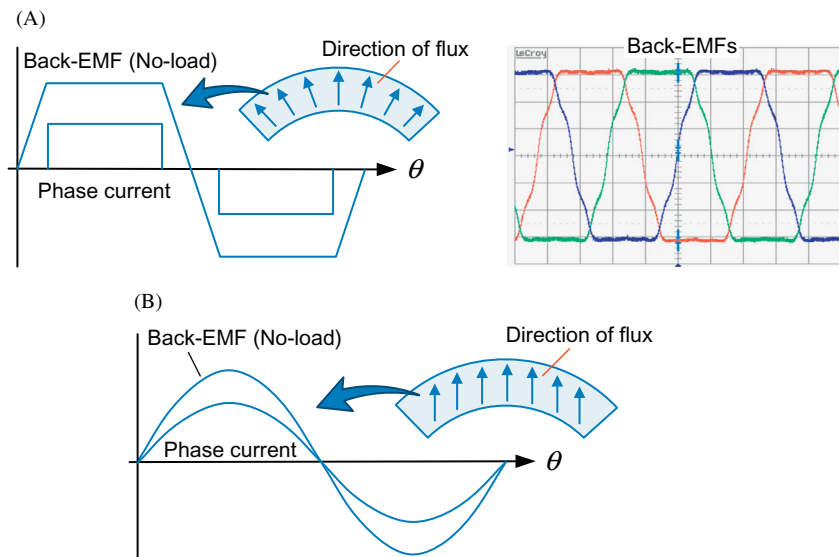
FIGURE 10.3

Comparison between (A) BLDC motors and (B) PMSMs.

When a BLDC motor with a trapezoidal back-EMF waveform is fed with a rectangular stator current, a constant torque can be developed. On the other hand, a PMSM is a type of AC motor with a sinusoidal back-EMF waveform, and thus its current should be a sinusoidal waveform for constant torque generation as shown in Fig. 10.3B.

A sinusoidal back-EMF waveform requires the magnetic flux density generated by the rotor magnets to be distributed sinusoidally along the air gap [2]. A PMSM is often referred to as *BLAC motor*, in contrast to BLDC motors.

Power density of a BLDC motor with a trapezoidal back-EMF waveform is 15% higher than that of a PMSM [3]. This is because the trapezoidal waveform has a higher fundamental component than the sinusoidal waveform, even though they have the same peak value. Besides the back-EMF waveform, there are several differences between BLDC motors and PMSMs. The comparison is listed in Table 10.1.

As shown in Fig. 10.4, a BLDC motor commonly uses concentrated stator windings, and quasi-square waveform current flows into them. In contrast, a PMSM usually uses distributed stator windings, into which the sinusoidal waveform current flows as shown in Chapter 3. However, recently, PMSMs often use concentrated windings due to their short end windings and simple structure suitable for automated manufacturing.

There is a clear difference in drive methods for these two motors. In the excitation of a three-phase BLDC motor, the phase currents flow only in two of the three-phase windings at a time and thus, each switch of the inverter always operates for a 120° conduction interval per fundamental operating cycle. By contrast, as described in Chapter 7, in a three-phase PMSM, the phase currents flow in all three-phase windings at a time and thus, each switch of the inverter always operates for a 180° conduction interval per fundamental operating cycle.

Table 10.1 Comparison Between BLDC Motors and PMSMs

	BLDC Motor	PMSM
Back-EMF	Trapezoidal waveform	Sinusoidal waveform
Stator winding	Concentrated winding	Distributed winding
Stator current	Quasi-square waveform	Sinusoidal waveform
Driving circuit	Inverter (120° conduction)	Three-phase inverter (180° conduction)
Drive method	Simple, using low-cost Hall effect sensors	Complex (using high-resolution position sensor such as an encoder or a resolver)
Torque ripple	Significant torque ripple	Nearly constant torque
System cost	Low cost	High cost
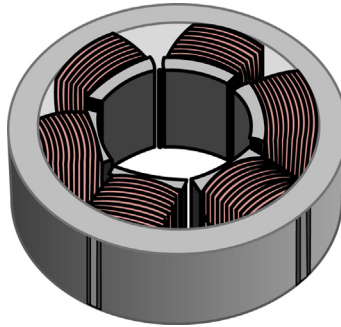
FIGURE 10.4

Concentrated stator windings of BLDC motors.

The BLDC motor drive is simple and inexpensive compared with the PMSM drive, which requires a complex method of the vector control as described in Chapter 5. However, the BLDC motors have a significant torque ripple during the phase commutation of changing an active switch, which will be explained later.

### 10.1.3 CONSTRUCTION OF BRUSHLESS DIRECT CURRENT MOTORS

BLDC motors can be categorized according to their number of stator windings: single-phase, two-phase, three-phase, and multi-phase.

Single-phase BLDC motors are widely used for appliances and small machines due to their simple structure, simple driving circuit, and low cost. However, such motors can rotate only in one direction. Furthermore, since they have a detent point where there is no starting torque, a motor design including an ancillary part is necessary for start-up. A reluctance torque is usually used as the starting torque, resulting in a large cogging torque. Single-phase BLDC motors are beneficial to small power applications below 10 W such as fans and blowers that require a low starting torque.

Multi-phase BLDC motors above four-phase can be mainly applied to aerospace and military applications requiring high reliability due to increased power density and fault-tolerance capability. Three-phase BLDC motors are the most widely used and our discussion will be limited to these motors in this book.

There are two BLDC motor designs which are classified in terms of magnetic flux direction: *radial-flux type*, where the flux from the rotor magnet crosses the air gap in a radial direction and *axial-flux type*, where the flux crosses the air gap in an axial direction as shown in Fig. 10.5.

Traditionally the radial-flux motors have been used almost exclusively. This type of motor can be either an *inner rotor type* or an *outer rotor type* as shown in Fig. 10.5A and B. As the most common type, the inner rotor design has an advantage of higher heat dissipating capacity, high torque-to-inertia ratio, and lower rotor inertia. Its common application is servo drives requiring a quick dynamic response.
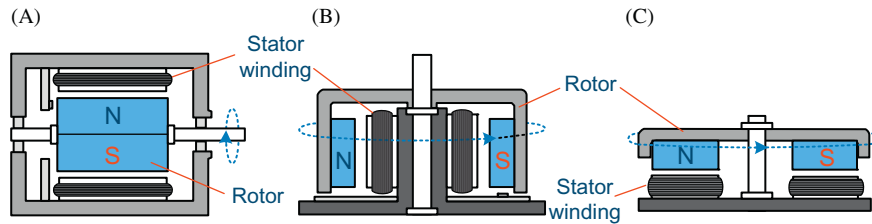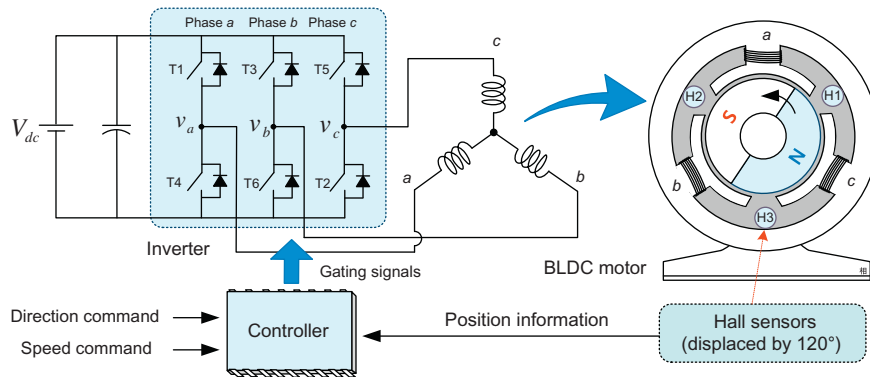
FIGURE 10.5

Classification of BLDC motors. (A) Radial-flux (inner rotor), (B) radial-flux (outer rotor), and (C) axial-flux.

Since the rotor is cylindrical in shape with a shaft on which the bearings are mounted, this type of motor can produce less vibration and acoustic noise. Outer rotor motors shown in Fig. 10.5B, in which the rotor magnets rotate around the stator windings located in the iron core of the motor, have relatively high rotor inertia. Thus this motor is favorable for systems requiring constant speed operation. The magnets affixed inside the yoke are beneficial to high-speed operation. The outer rotor motor can use more magnetic material than the inner rotor device, which means it is capable of more flux even though lower energy product magnets are used. These days, this type of motor is increasingly being used in many applications such as computer disk drives, cooling fans, and washing machines.

In the axial-flux motors shown in Fig. 10.5C, a disc rotor with magnets whose flux is in an axial direction rotates facing the stator. Permanent magnets are glued to the surface of the rotor. In this design topology small motors often have coreless stator windings mounted to a nonmagnetic substrate or slotless stator windings mounted to an iron core without slots. The primary advantage of such a technology is that it has a very low ripple torque and acoustic noise since the cogging torque associated with typical iron core motors can be eliminated due to no variations in reluctance. Their relatively high rotor inertia is favorable to constant speed operation. However, due to increased effective air gap, the available flux is somewhat low. Common applications are VCR and CD player drives. This axial-flux motor with a slimmer structure of shorter axial length is very suitable for applications in which the axial length of the motor is the limiting design parameter, or the motor is directly coupled to the driven load. Such applications include electrical vehicles in-wheel motors and elevator motors.

10.2 DRIVING PRINCIPLE OF BRUSHLESS DIRECT CURRENT MOTORS

The basic driving principle of the BLDC motor is to change the phase windings, which should be excited according to the position of permanent magnet on the

**FIGURE 10.6**

BLDC motor drive system.

rotor for producing a continuous torque. To implement this function, information on the rotor magnet position is indispensable. The position sensing is commonly achieved with Hall effect sensors.

A two-pole three-phase Y-connected BLDC motor drive system is shown in Fig. 10.6. Three Hall effect sensors are displaced from each other by 120 electrical degrees on the stator to detect the magnetic field flux produced from the rotor magnets. Three output signals of Hall effect sensors enable us to recognize the rotor position divided into six different sections. Accordingly, a basic drive (often called *six-step drive*) to complete one electrical cycle consists of six different sections.

HALL EFFECT SENSOR

The Hall effect sensor is a device that can detect magnetic field by making use of the Hall effect on the semiconductor material. As shown in the following figure, when a current I_H is flowing through the plate of semiconductor material (called Hall element) and a magnetic field density B passes through the plate, a voltage V_H is generated in response to the magnetic field by the Hall effect as

$$V_H = \frac{R_H}{d} I_H B \text{ (V)} \quad (R_H: \text{Hall constant}, d: \text{width of an element})$$
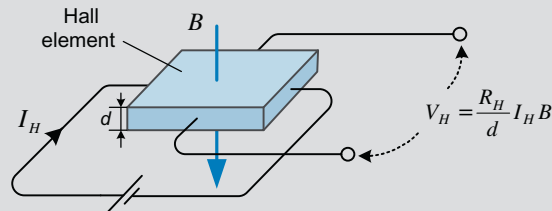

(*Continued*)

HALL EFFECT SENSOR (CONTINUED)

From measuring the voltage V_H, the position and polarity of a magnetic field can be detected. Thus the Hall effect sensors are used to detect the rotor position of permanent magnet motors such as BLDC motors and PMSMs. They are also used for current sensors as shown in the following figure. From measuring the output voltage of the Hall effect sensor, the magnitude and the direction of the current, which produces the magnetic field, can be detected.
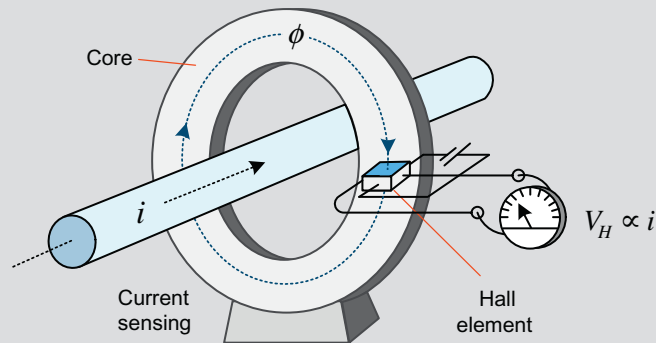
The switching sequence for the six-step drive is illustrated in Fig. 10.7. In the BLDC motor drive, only two of the three-phase windings are excited, while the other winding is left unexcited. This is the difference from the inverter drive method for AC motors, which is mentioned in Chapter 7. Rotor position feedback signals can be used to determine which two of the three-phase windings should be excited to produce the continuous torque at each instant. As a driving circuit, a three-phase inverter is used to flow the current into the required two-phase windings. In the inverter for a BLDCM drive as shown in Fig. 10.7, switching devices of only two phases work at any given instant. Accordingly, each switching device has a 120° conduction interval. In the six-step drive, a changeover of an active switch is done to the switch of the other phase, and thus a dead time is not required for short-circuit protection in the inverter.

Fig. 10.8 illustrates Hall effect sensor signals (H_1, H_2, H_3) with respect to back-EMFs of stator windings in the six-step drive as shown in Fig. 10.7, and the relationship between the sensor signals and the phase currents. Here, assume that each sensor outputs a digital high level for the north pole, whereas it outputs a low level for the south pole. From the sensor signals, the excited phase winding, i.e., an active phase winding, should be changed every 60 electrical degrees of rotation for producing a continuous torque. The transition of an active phase winding is called *commutation*. For the reverse rotation, the switching sequence with respect to Hall effect sensor signals should be altered.
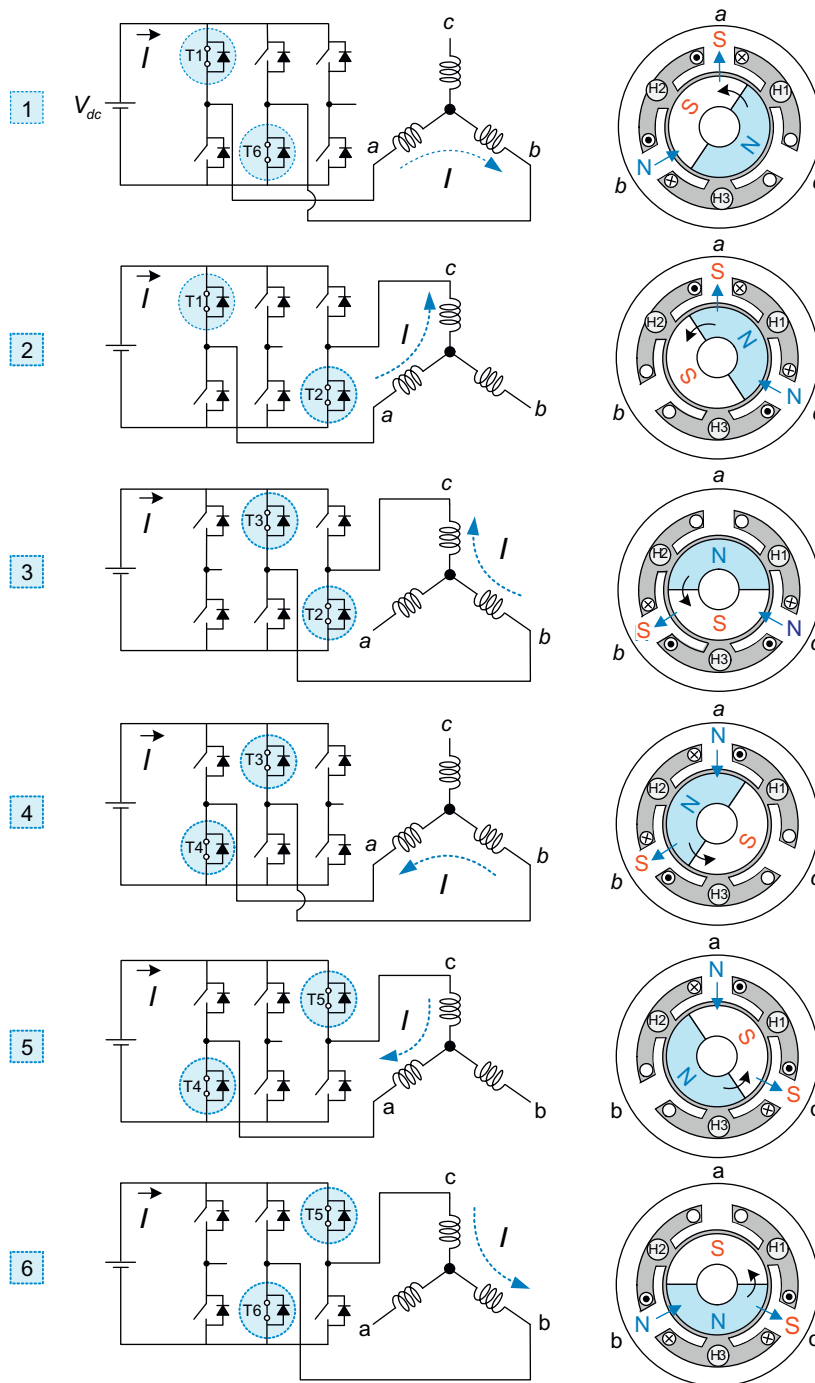
FIGURE 10.7

Switching sequence for two-pole three-phase BLDC motor.
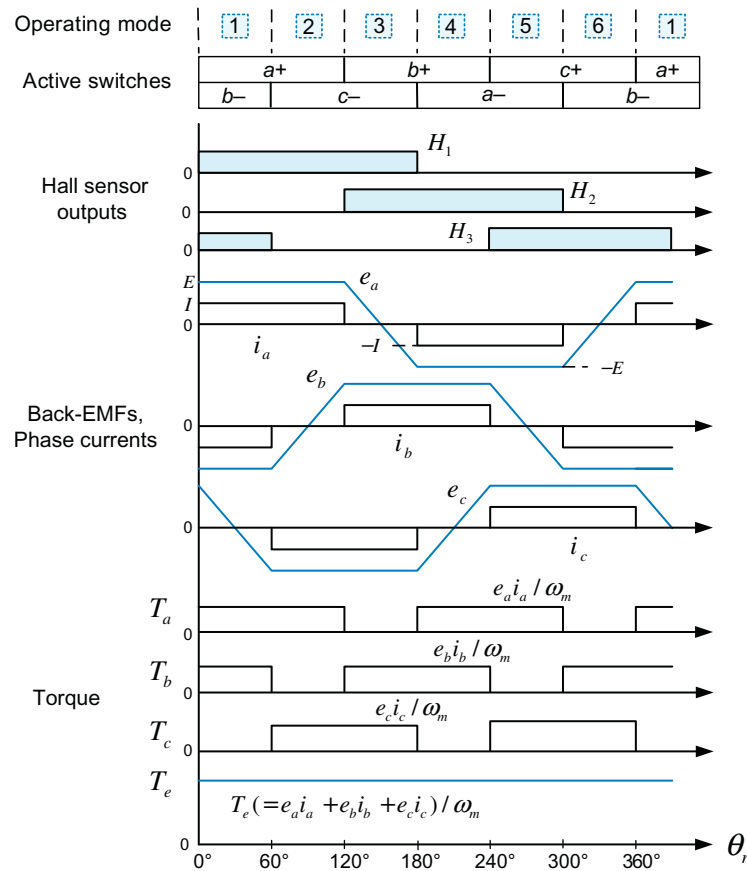
FIGURE 10.8

Driving principle of three-phase BLDC motor.

10.3 MODELING OF BRUSHLESS DIRECT CURRENT MOTORS

In this section, we will derive the mathematical model of a three-phase BLDC motor [3]. The model of a BLDC motor is similar to that of a PMSM due to their structural similarity.

10.3.1 VOLTAGE EQUATIONS

Let us consider a two-pole three-phase BLDC motor as shown in Fig. 10.9. Similar to AC motors examined in Chapter 4, the voltage equation for the stator windings of a BLDC motor can be expressed as
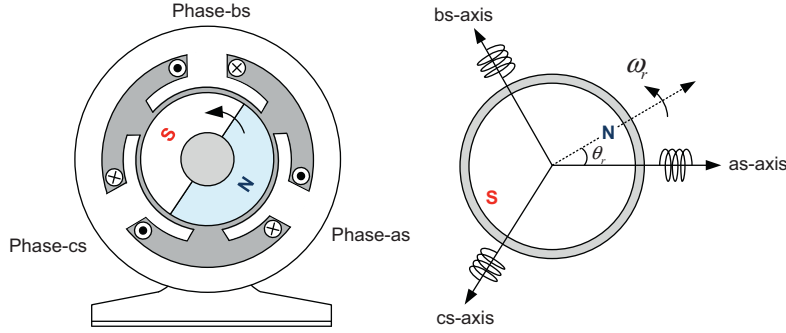
FIGURE 10.9

Windings of a two-pole three-phase BLDC motor.

$$v_{abcs} = R_s i_{abcs} + \frac{d\lambda_{abcs}}{dt} \tag{10.1}$$

where the stator voltage $v_{abcs} = [v_{as} v_{bs} v_{cs}]^T$, the stator current $i_{abcs} = [i_{as} i_{bs} i_{cs}]^T$, the stator flux linkage $\lambda_{abcs} = [\lambda_{as} \lambda_{bs} \lambda_{cs}]^T$, and the stator resistance $R_s = \begin{bmatrix} R_s & 0 & 0 \\ 0 & R_s & 0 \\ 0 & 0 & R_s \end{bmatrix}$.

The flux linkage λ_{abcs} of the stator windings consists of $\lambda_{abcs(s)}$ due to the stator currents i_{abcs} and $\lambda_{abcs(f)}$ due to the permanent magnet as

$$\lambda_{abcs} = \lambda_{abcs(s)} + \lambda_{abcs(f)} \tag{10.2}$$

Substituting Eq. (10.2) into Eq. (10.1) gives the following stator voltage equation.

$$v_{abcs} = R_s i_{abcs} + \frac{d\lambda_{abcs}}{dt} = R_s i_{abcs} + \frac{d\lambda_{abc(s)}}{dt} + e_{abcs} \tag{10.3}$$

where the back-EMF due to the magnet flux is expressed as $e_{abcs} = d\lambda_{abc(f)}/dt$ and is also given as

$$e_{abcs} = \begin{bmatrix} e_{as} \\ e_{bs} \\ e_{ac} \end{bmatrix} = \omega_m \begin{bmatrix} \lambda_{asf} \\ \lambda_{bsf} \\ \lambda_{csf} \end{bmatrix} = \omega_m \lambda_f \begin{bmatrix} f(\theta_r) \\ f(\theta_r - 120°) \\ f(\theta_r - 240°) \end{bmatrix} \tag{10.4}$$

where $\lambda_f (= N\phi_f)$ is the amount of the magnet flux ϕ_f linking N turns of the stator windings, $f(\theta_r)$ is a unit function representing the waveform of the back-EMF and θ_r is the rotor position.

The unit function for the trapezoidal back-EMF waveform of a BLDC motor can be expressed as

$$f(\theta_r) = \begin{cases} 6\theta_r/\pi & (0 \le \theta_r < \pi/6) \\ 1 & (0 \le \theta_r < \pi/6) \\ -6\theta_r/\pi & (0 \le \theta_r < \pi/6) \\ -1 & (0 \le \theta_r < \pi/6) \\ 6\theta_r/\pi - 12 & (0 \le \theta_r < \pi/6) \end{cases} \tag{10.5}$$

The stator flux linkage $\boldsymbol{\lambda}_{abcs(s)}$ due to the stator currents is given by

$$\boldsymbol{\lambda}_{abcs(s)} = \boldsymbol{L}_s \boldsymbol{i}_{abcs} = \begin{bmatrix} L_{aa} & L_{ab} & L_{ac} \\ L_{ba} & L_{bb} & L_{bc} \\ L_{ca} & L_{cb} & L_{cc} \end{bmatrix} \begin{bmatrix} i_{as} \\ i_{bs} \\ i_{cs} \end{bmatrix} \tag{10.6}$$

As can be seen in Section 4.1.1, for symmetry three-phase windings, the self-inductances are all the same and the mutual-inductances are all the same as in the following

$$L_{aa} = L_{bb} = L_{cc} = L_s = L_{ls} + L_m \tag{10.7}$$

$$L_{ab} = L_{ac} = L_{ba} = L_{bc} = L_{ca} = L_{cb} = -\frac{1}{2}L_m = M \tag{10.8}$$

where $L_{\alpha\beta}(=\lambda/i_\beta)$ expresses the winding inductance, which is the ratio of the flux linkage λ of the winding α to the current i_β that produces the flux. Here, the values of leakage inductance L_{ls} and magnetizing inductance L_m are the same as those of a PMSM described in Chapter 4.

From Eqs. (10.6)−(10.8), the stator voltage equation is rewritten as

$$\boldsymbol{v}_{abcs} = \boldsymbol{R}_s \boldsymbol{i}_{abcs} + \boldsymbol{L}_{abcs} \frac{d\boldsymbol{i}_{abc(s)}}{dt} + \boldsymbol{e}_{abcs} \tag{10.9}$$

$$\begin{bmatrix} v_{as} \\ v_{bs} \\ v_{cs} \end{bmatrix} = \begin{bmatrix} R_s & 0 & 0 \\ 0 & R_s & 0 \\ 0 & 0 & R_s \end{bmatrix} \begin{bmatrix} i_{as} \\ i_{bs} \\ i_{cs} \end{bmatrix} + \begin{bmatrix} L_s & M & M \\ M & L_s & M \\ M & M & L_s \end{bmatrix} \frac{d}{dt} \begin{bmatrix} i_{as} \\ i_{bs} \\ i_{cs} \end{bmatrix} + \begin{bmatrix} e_{as} \\ e_{bs} \\ e_{cs} \end{bmatrix} \tag{10.10}$$

here, since $i_{as} + i_{bs} + i_{cs} = 0$, the mid-term of Eq. (10.10) is reduced as

$$\frac{d}{dt}[L_s i_{as} + M i_{bs} + M i_{cs}] = \frac{d}{dt}[L_s i_{as} - M i_{as}] \tag{10.11}$$

Thus Eq. (10.10) becomes the following voltage equations.

$$\begin{bmatrix} v_{as} \\ v_{bs} \\ v_{cs} \end{bmatrix} = \begin{bmatrix} R_s & 0 & 0 \\ 0 & R_s & 0 \\ 0 & 0 & R_s \end{bmatrix} \begin{bmatrix} i_{as} \\ i_{bs} \\ i_{cs} \end{bmatrix} + \begin{bmatrix} L_s - M & 0 & 0 \\ 0 & L_s - M & 0 \\ 0 & 0 & L_s - M \end{bmatrix} \frac{d}{dt} \begin{bmatrix} i_{as} \\ i_{bs} \\ i_{cs} \end{bmatrix} + \begin{bmatrix} e_{as} \\ e_{bs} \\ e_{cs} \end{bmatrix}$$
$$\tag{10.12}$$

Voltage Equations of a Brushless Direct Current Motor

$$v_{as} = R_s i_{as} + (L_s - M)\frac{di_{as}}{dt} + e_{as} \tag{10.13}$$

$$v_{bs} = R_s i_{bs} + (L_s - M)\frac{di_{bs}}{dt} + e_{bs} \tag{10.14}$$

$$v_{cs} = R_s i_{cs} + (L_s - M)\frac{di_{cs}}{dt} + e_{cs} \tag{10.15}$$

Unlike AC motors that use the $d-q$ axes reference frame to facilitate their control, BLDC motors directly use three-phase abc quantities for their control. The $d-q$ transformation is necessary for the sinusoidal quantities. Since currents, flux, and back-EMFs of a BLDC motor are nonsinusoidal quantities, the $d-q$ transformation on the BLDC motor is meaningless.

10.3.2 **TORQUE EQUATION**

The output torque T_e of a three-phase motor is generally calculated from the output power P_e and the mechanical angular velocity ω_m as

$$P_e = e_{as} i_{as} + e_{bs} i_{bs} + e_{cs} i_{cs} \tag{10.16}$$

$$T_e = \frac{P_e}{\omega_m} = \frac{e_{as} i_{as} + e_{bs} i_{bs} + e_{cs} i_{cs}}{\omega_m} \tag{10.17}$$

here, the mechanical angular velocity $\omega_m = \omega_r / P$. In addition, ω_r is the electrical angular velocity and P is the number of pole.

From this torque equation, we can readily see that the phase current is needed to be in phase with the back-EMF to produce the maximum torque. The drive shown in Fig. 10.8 satisfies this requirement for maximum torque production.

Now we will discuss the output torque of a three-phase BLDC motor driven by the 120° conduction method. In a BLDC motor, the currents of two-phase windings are the same in magnitude but flow in the reverse direction except during the commutation interval. As an example, consider Section 1 shown in Fig. 10.8. In that section, $i_{as} = I$, $i_{bs} = -I$, $i_{cs} = 0$ and $e_{as} = E$, $e_{bs} = -E$. Since the phase current is in phase with the back-EMF, the torque of Eq. (10.17) can be simply expressed as the product of the magnitudes of the phase current and back-EMF as

$$T_e = \frac{e_{as} i_{as} + e_{bs} i_{bs} + e_{cs} i_{cs}}{\omega_m} = 2\frac{EI}{\omega_m} \tag{10.18}$$

For the remaining sections, we can obtain the same result.

If I and E are constant values, the output torque of Eq. (10.18) becomes a constant value. However, if the back-EMF is not an ideal trapezoidal waveform,

there is a torque ripple even though the BLDC motor is fed with constant stator currents. For a BLDC motor having arbitrary back-EMF waveforms of Eq. (10.4), the output torque can be expressed as

$$T_e = \lambda_f [i_{as} f(\theta) + i_{as} f(\theta - 240°) + i_{as} f(\theta - 120°)] \tag{10.19}$$

10.3.2.1 Torque ripple during the commutation

Even though the back-EMF is an ideal trapezoidal waveform, a torque ripple may occur due to the current ripple introduced during the commutation of phase currents [4−8]. This torque ripple may be a major obstacle in applying a BLDC motor for high-performance motor drives. Below is a description on the causes of the torque ripple during the commutation of phase currents.

Consider the commutation of the phase current from Section 2 to Section 3 in Fig. 10.10. The stator current during the commutation is assumed to be constant and equal to *I*. The magnitude of back-EMF is also supposed to remain as a constant value *E*.

In Section 2, the stator current *I* flows from phase *as* to phase *cs*, while in Section 3, the current *I* flows from phase *bs* to phase *cs*. Thus the current is commutated from phase *as* to phase *bs* during the transition from Section 2 to Section 3. In this case the phase *as* current i_{as} decreases to zero, while the phase *bs* current increases to its final value *I*. Meanwhile, the phase *cs* current i_{cs}, i.e.,
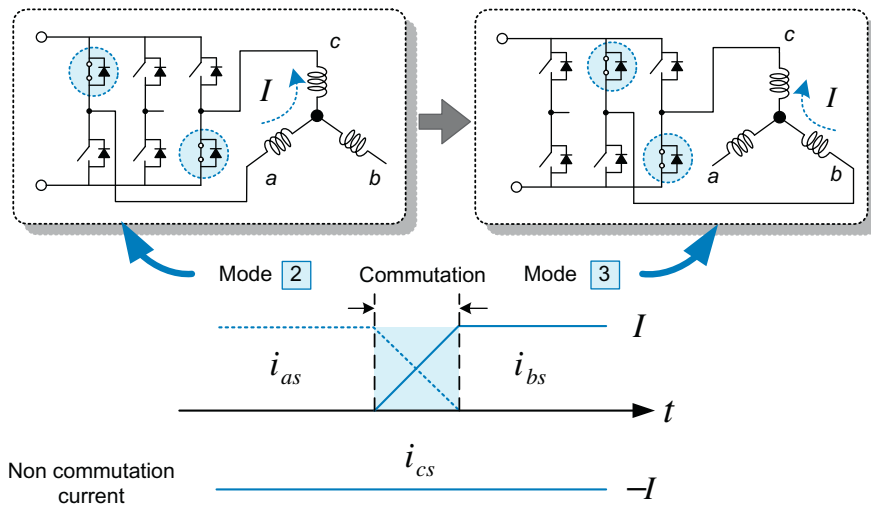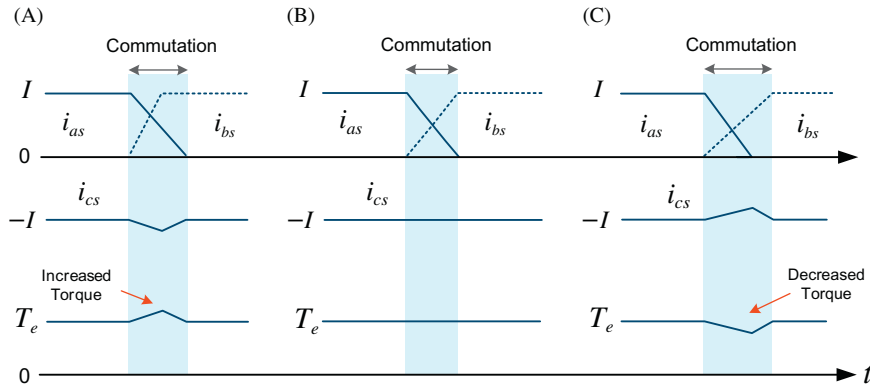

FIGURE 10.10

Commutation of phase currents.

noncommutation current, remains unchanged. During the transition from Section 2 to Section 3, $e_{as} = e_{bs} = E$, $e_{cs} = -E$. Thus the output torque of Eq. (10.18) can be expressed as

$$T_e = \frac{e_{as}i_{as} + e_{bs}i_{bs} + e_{cs}i_{cs}}{\omega_m} = \frac{E(i_{as} + i_{bs}) - Ei_{cs}}{\omega_m} = -\frac{2E}{\omega_m}i_{cs} \qquad (10.20)$$

From Eq. (10.20), it can be readily seen that, during the commutation, the torque is proportional to the noncommutation current i_{cs}. If the noncommutation current i_{cs} remains a constant value during the commutation, then the torque also becomes a constant value.

During the commutation, it takes time to change the current due to the winding inductance. If the decreasing rate of the phase as current is equal to the increasing rate of the phase bs current, then $i_{as} + i_{bs} = I$, so the phase cs current i_{cs} remains at a constant value, $-I$. However, in practice, these two rates of change are usually not equal to each other due to the back-EMF, DC-link voltage, time constant of windings, etc. Accordingly, the noncommutation current cannot remain as a constant value, resulting in a torque ripple. For example, Fig. 10.11 shows that the rate of change of the current varies according to the back-EMF and DC-link voltage [4].

Fig. 10.11A shows that the phase bs current reaches the final value I before the phase as current reduces to zero. Hence, the noncommutation current, the phase cs current i_{cs}, becomes larger than I, resulting in an increase in the torque. On the other hand, Fig. 10.11C shows that the phase as current reduces to zero before the phase bs current reaches the final value, I. In this case the noncommutation current, phase cs current i_{cs}, becomes smaller than I, resulting in a decrease in the torque. Fig. 10.11B shows an ideal case where the phase as current reduces
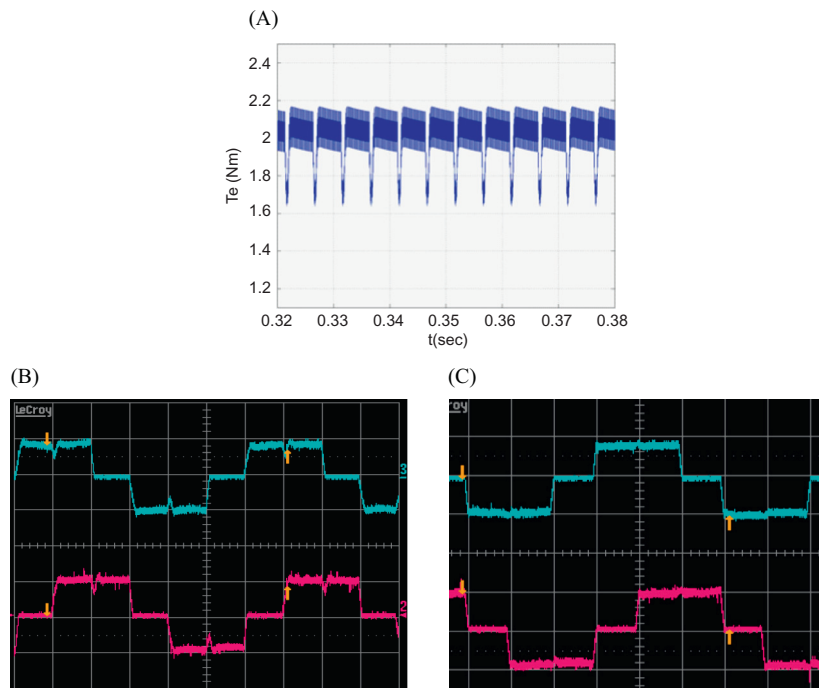

FIGURE 10.11

Phase currents during commutation in different cases. (A) low-speed ($V_{dc} > 4E$), (B) mid-speed ($V_{dc} = 4E$), and (C) high-speed ($V_{dc} < 4E$).

to zero at the same time the phase *bs* current reaches the final value *I*. In this case the noncommutation current remains constant, and thus results in the constant torque.

For this reason, whenever the winding current is commutated from one phase to another, a ripple in the output torque is generated. Thus this ripple of the torque occurs six times per cycle. The magnitude of the torque ripple depends on the operating current level and the operating speed. This is also different according to the pulse width modulation (PWM) techniques used in a driving inverter. Fig. 10.12A and B shows output torque and phase currents for the case shown in Fig. 10.11C. Commutation torque ripples produce noise and degrade speed control characteristics especially at low speeds. Thus many methods to reduce this torque ripple have been developed [4−8]. As an example, Fig. 10.12C shows that the ripple of the phase currents (thus, torque) is eliminated by using a commutation ripple compensation in which the motor input voltage is adjusted to equalize the rate of change of the current during the commutation [8]


FIGURE 10.12

Ripple of output torque and phase currents. (A) output torque, (B) phase current (without compensation), and (C) with compensation.
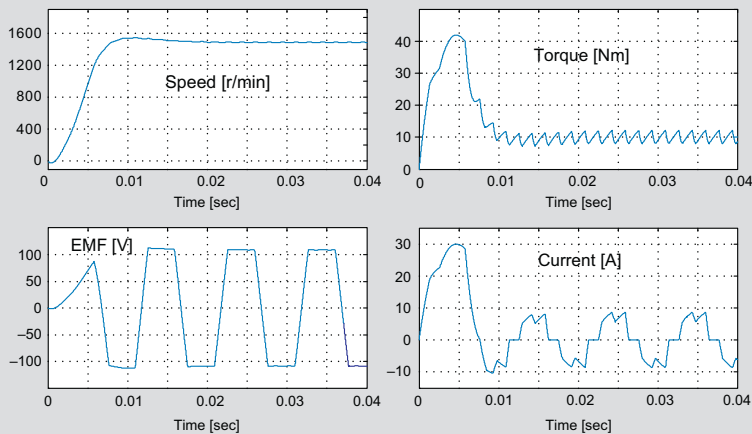
MATLAB/SIMULINK SIMULATION: BRUSHLESS DIRECT CURRENT MOTOR

The six-step drive for 4-pole, 300-V BLDC motor is simulated by using a permanent magnet synchronous machine block in SimPowerSystems/Machines library and Mosfet blocks in SimPowerSystems/Power Electronics library.

• Overall diagram for simulation

Basic BLDCM Drive System
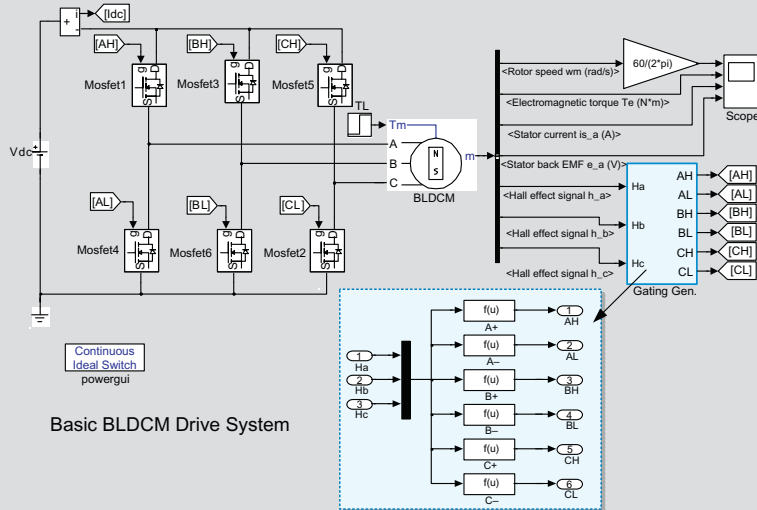
• Simulation results

10.4 **CONTROL OF BRUSHLESS DIRECT CURRENT MOTORS**

As can be seen in the Section 10.2, we can operate a BLDC motor easily by a proper commutation of phase currents based on the information of the rotor position. Similar to a DC motor, the operating speed of a BLDC motor is proportional to the voltage applied to the motor, and thus its speed can be controlled by adjusting the applied voltage.
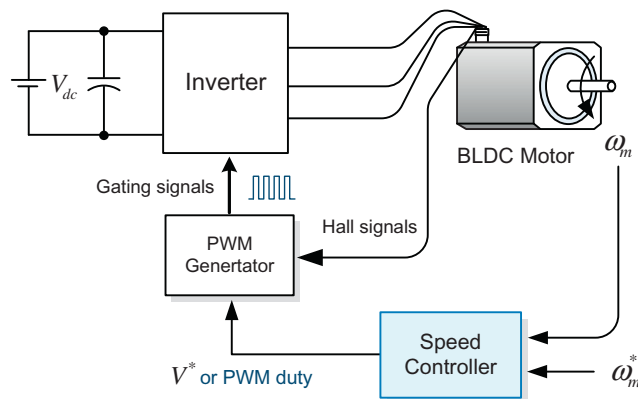
10.4.1 **SPEED CONTROL**

The simplest speed control system to control the speed of a BLDC motor is shown in Fig. 10.13. A proportional−integral (PI) controller as mentioned in Chapter 2, is commonly used for the speed control. This PI speed controller outputs the motor voltage reference (or PWM duty) as

$$V^* = \left(K_P + \frac{K_i}{s}\right)\cdot(\omega_m^* - \omega_m) \tag{10.21}$$

where K_P and K_i are the proportional and integral gains of the PI speed controller, respectively.

This reference voltage is generated by a PWM technique and then applied to the BLDC motor. This speed control system is simple but has a big problem. In this method, the motor current is hard to control within a proper range. This is because when a speed command is changed, the voltage reference may be changed largely. Thus we cannot expect to obtain a good dynamic response of the speed control. Moreover, this may incur a large transient current more than the rated current, which may lead to a shutdown of the drive system.

FIGURE 10.13

Speed control system of a BLDC motor.
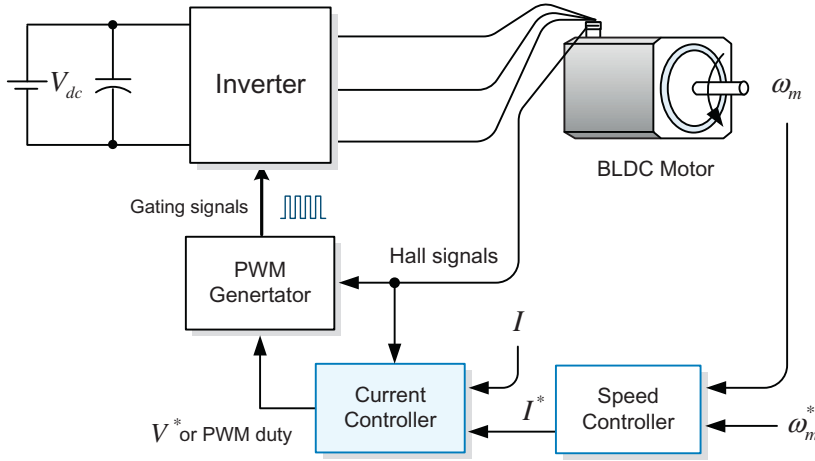
FIGURE 10.14

Speed control system based on the motor current.

To obtain a better dynamic response of the speed control, it is necessary to control the speed by controlling the torque or current of the BLDC motor. An enhanced speed control system based on the current control is shown in Fig. 10.14. Compared to the previous system of Fig. 10.13, this system includes a current controller to control the speed by regulating the current (thus, torque). In this case, the output of the PI speed controller becomes the motor current reference and a current sensor is needed to measure the actual motor current for the current control.

For AC motor drives, both the amplitude and phase of three-phase currents are instantaneously regulated to control the torque. However, for the BLDC motor drive, only the amplitude of phase currents needs to be regulated. This is because, as we can see in Eq. (10.18), the developed torque is proportional to the amplitude of the phase current. In addition, when controlling the amplitude of the current, we may regulate three-phase currents individually like in the current control of AC motors. However, since the amplitude of the phase current of a BLDC motor is proportional to the DC-link side current I_{dc}, the amplitude of the phase current is commonly controlled by regulating I_{dc}. In this case, the drive system needs only one current sensor at the DC-link side, and thus is more cost-effective.

Fig. 10.15 shows the speed control system using the regulation of the DC-link current. In this system, the speed controller produces the DC-link current reference as

$$I_{dc}^* = \left(K_{ps} + \frac{K_{is}}{s} \right) \cdot (\omega_m^* - \omega_m) \tag{10.22}$$

here, K_{ps} and K_{is} are the proportional and integral gains of the PI speed controller, respectively. These values can be determined from the gains selection procedure of a PI speed controller that was explained in Section 2.7.
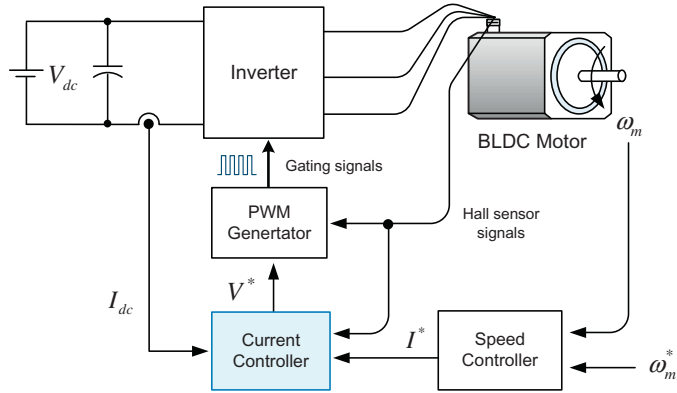
FIGURE 10.15

Speed control system using the regulation of the DC-link current.

To achieve the DC-link current reference I_{dc}^* produced by the speed controller, switching signals for an inverter are usually generated by a hysteresis regulation technique or a PWM technique.

10.4.2 **CURRENT CONTROL**

As can be seen from Chapter 6, the hysteresis technique is simply implemented and gives an excellent transient response because it directly determines the switching states from the current error. However, the hysteresis technique has a major drawback of varying the switching frequency with operating conditions, such as the back-EMF, load condition, etc. Thus, to have a constant switching frequency, a PWM technique is commonly used, but it is inferior to the hysteresis technique in performance.

In the case of using a PWM technique, a motor voltage reference (or PWM duty) is generated by the PI current controller from an error between the current command I_{dc}^* and the actual current as

$$V^* = \left(K_{pc} + \frac{K_{ic}}{s} \right) \cdot (I_{dc}^* - I_{dc}) \tag{10.23}$$

here, K_{pc} and K_{ic} are the proportional and integral gains of the current controller, respectively. These values can also be determined from the gains selection procedure of a PI current controller that was explained in Chapter 2.

Finally, the actual active switches are determined by combining the PWM switching signals with the operating mode signal decoded by using Hall effect sensor signals.
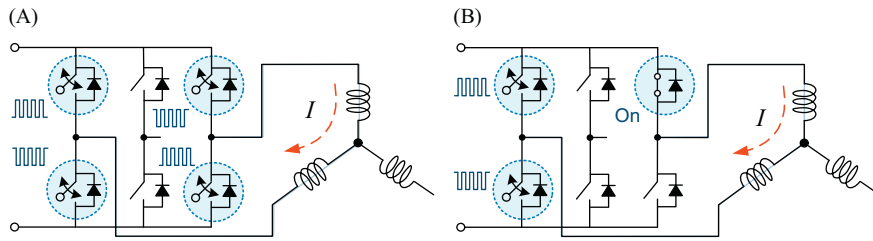
FIGURE 10.16

PWM techniques. (A) bipolar switching and (B) unipolar switching.

10.5 PULSE WIDTH MODULATION TECHNIQUES

In BLDC motor drives, there are two conventional PWM techniques for generating a motor applied voltage the as shown in Fig. 10.6: *bipolar switching method* and *unipolar switching method* [9−10]. These are similar to the PWM techniques of the H-bridge circuit for DC motor drives in Section 2.8. This similarity is due to the facts that switches of only two phases are being driven in the three-phase inverter for BLDC motor drives. However, there are several variations for the unipolar switching method. Now let us examine these PWM techniques.

10.5.1 BIPOLAR SWITCHING METHOD

In the bipolar switching method, a PWM signal is applied to all switches of two phases as shown in Fig. 10.16A. By contrast, in the unipolar switching method as shown in Fig. 10.16B, a PWM signal is applied to the switches of only one phase while one switch of the other phase is kept at an on-state. The bipolar method is simple and can give a better transient response because $+V_{dc}$ or $-V_{dc}$ is applied across the phase winding. However, the current ripple (thus, torque ripple) and switching losses are greater than those of the unipolar switching method. The PWM gating signals by the bipolar switching method are shown in Fig. 10.17.

10.5.2 UNIPOLAR SWITCHING METHOD

In the unipolar switching method, switching losses can be reduced because the PWM signal is applied to the switches of only one phase. In addition, since the applied voltage to the phase windings is 0 and $+V_{dc}$ or 0 and $-V_{dc}$, the current ripple is half of that of the bipolar switching method. Due to these advantages, the unipolar switching method is more widely used for BLDC motor drives. However, this method is complicated and has a slower response than the bipolar switching method. In addition, circulating currents may occur in the inactive phase windings. Thus this method is less favorable for precision servo drives.
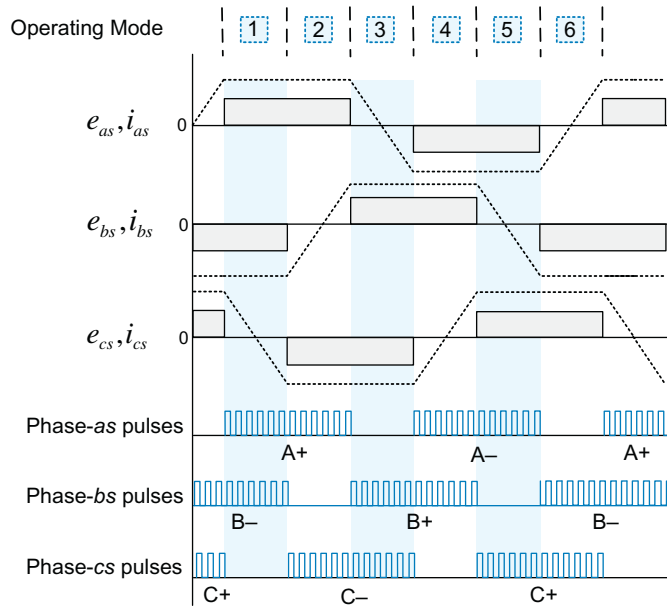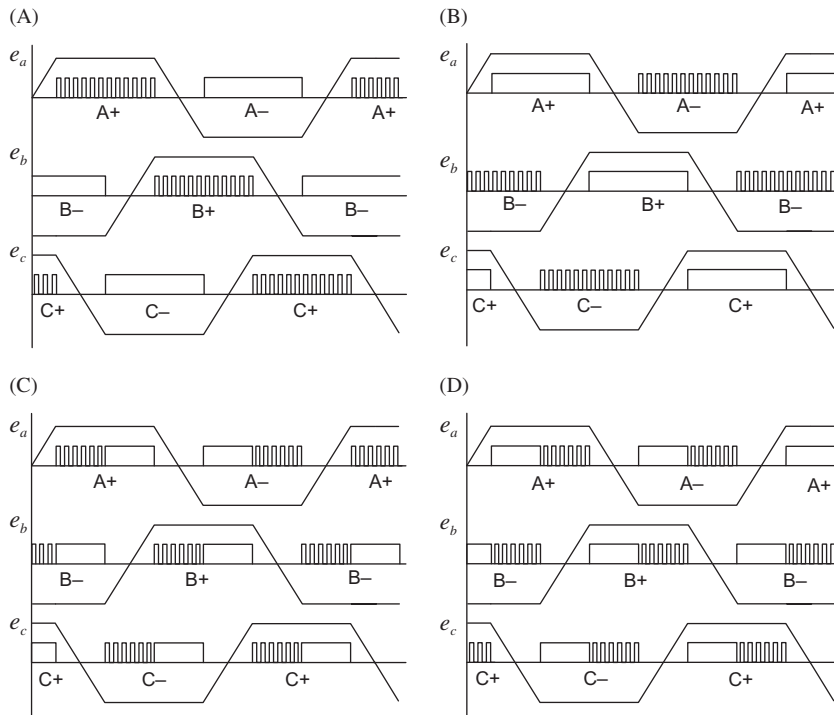
FIGURE 10.17

Bipolar switching method.

The unipolar switching method is also divided into several schemes according to the executing switch. In the *upper switch PWM scheme* in Fig. 10.18A, the PWM signal is applied to the upper switch only while the lower switch is kept at an on-state. On the other hand, in the *lower switch PWM scheme* in Fig. 10.18B, the PWM signal is applied to the lower switch only while the upper switch is kept at an on-state. In these two schemes, however, the utilization of switches and switching losses are biased because only one specific switch makes a continuous switching.

As types of improved schemes through uniform switching, there are *on-going PWM scheme* and *off-going PWM scheme* [9]. In the on-going PWM scheme shown in Fig. 10.18C, the PWM signal is applied to each switch during the front 60° part of the 120° conduction interval. In the off-going PWM scheme shown in Fig. 10.18D, the PWM signal is applied to each switch during the latter 60° part of the 120° conduction interval.

These unipolar PWM schemes have a disadvantage of having an increased ripple torque and a lowered efficiency because of ripple current, which occurs in the inactive phase windings due to diode freewheeling. The magnitude and direction of the ripple current depends on the PWM schemes. We can see, from Fig. 10.19, the ripple current during the inactive interval for unipolar PWM schemes that were explained above. In addition, the bipolar switching method has no ripple current due to no diode freewheeling. The PWM scheme, which is called

FIGURE 10.18

Different schemes of the unipolar switching method. (A) upper switch PWM, (B) lower switch PWM, (C) on-going PWM, and (D) off-going PWM.
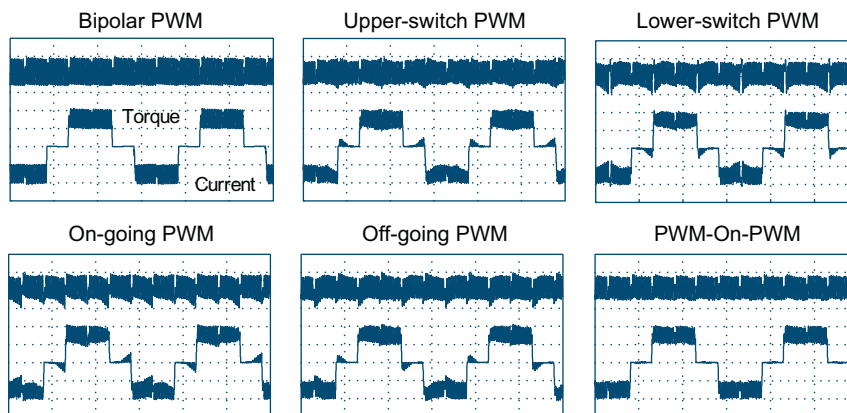
FIGURE 10.19

Comparison of phase and torque for PWM schemes.

PWM_ON_PWM scheme, to eliminate diode freewheeling in the inactive phase has been developed [10]. In this scheme the switches are in PWM mode in the beginning 30° and the last 30° zones, and in continuous on-state in the middle 60° zone of the 120° conduction interval.

As it can be seen from above, characteristics such as ripple torque during commutation, switching losses, and sensorless control performance vary according to different unipolar PWM schemes. The torque ripple comparison of PWM schemes is shown in Fig. 10.19.

10.6 SENSORLESS CONTROL OF BRUSHLESS DIRECT CURRENT MOTORS

As described in the Section 10.2, Hall effect sensors for obtaining the rotor position are indispensable for BLDC motor drives. However, since the position sensors increase the cost and size of the motor and reduce the reliability of a drive system, a BLDC motor drive without position or speed sensors is becoming more popular.

Various sensorless methods for BLDC motors have been seen in the literature [11−15]. One well-known method is the back-EMF-based method [11]. There is also a method based on the current of the freewheeling diodes of the noncommutation phase [13] and a method based on a flux observer. Among these, we will explore the back-EMF-based method, which is the most widely used for low-cost applications such as fan, pump, and compressor drives due to its easy principle and implementation.

10.6.1 SENSORLESS CONTROL BASED ON THE BACK-ELECTROMOTIVE FORCE

The back-EMF of a motor includes information on the magnetic flux. Thus the rotor position can be obtained by detecting the back-EMF. It is hard to measure the back-EMF of AC motors because all three windings are excited at all times. On the other hand, in three-phase BLDC motor drives, since only two of the three-phase windings are conducting at a time, the back-EMF appears in the open winding of the nonconducting phase. Thus the back-EMF can be detected by sensing the voltage of the nonconducting phase. In BLDC motors, we can consider that the nonconducting phase winding plays the role of a sensor to detect the position.

In this case, there is no need to detect the whole waveform of the back-EMF. Instead, the commutation instants can be identified by detecting only the zero crossing point (ZCP) of the back-EMF. From Fig. 10.20, we can easily see that the back-EMFs of a nonconducting phase always pass through zero (see the parts arrows are indicating). For example, in Section 2 where phase *as* and *cs* are conducting and phase *bs* is nonconducting, we can identify that the back-EMF of
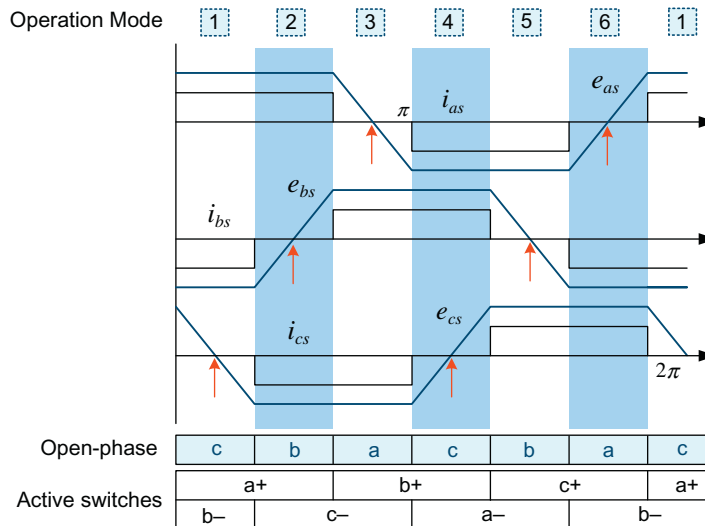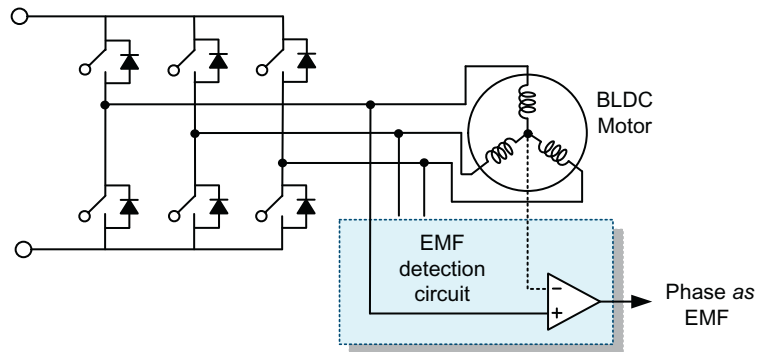
FIGURE 10.20

ZCPs of the back-EMF.

phase *bs* passes through zero. In addition, it can be seen that the commutations happen 30 electrical degrees after the ZCPs of the back-EMFs.

Therefore, without any position sensor, the phase commutation is made possible by detecting the ZCPs of the back-EMFs.

For three-phase Y-connected windings, the back-EMF across a phase can be obtained directly from measuring the phase terminal voltage referred to the neutral point of windings as shown in Fig. 10.21. However, in most cases, the neutral point of windings is not accessible. Thus the most commonly used method is to create a virtual neutral point by using the three-phase terminal voltages.

The back-EMF-based methods have the following problems. When measuring the terminal voltage, a large amount of electrical noise is induced on the sensed terminal voltage due to PWM switching signals driving the motor. Low-pass filters are usually used to remove unwanted switching noise, but the phase delay of the low-pass filter causes a commutation delay at high speeds. In addition, attenuation by a voltage divider will be required to lower the level of the sensed signal to an acceptable range of the control circuit. This lowers the signal-to-noise ratio at low speeds, resulting in degradation of low-speed operation performance. Moreover, the commutation happens 30 electrical degrees after the ZCPs of the back-EMFs. It is hard to obtain commutation instants precisely when the operating speed is changing. To improve these problems, the back-EMF integration the third harmonic voltage integration, and the method detecting the conducting current of the freewheeling diodes in the unexcited phase have been presented [13−14]. However, they still have a low accuracy problem at low speeds.

FIGURE 10.21

Back-EMF detection circuit.
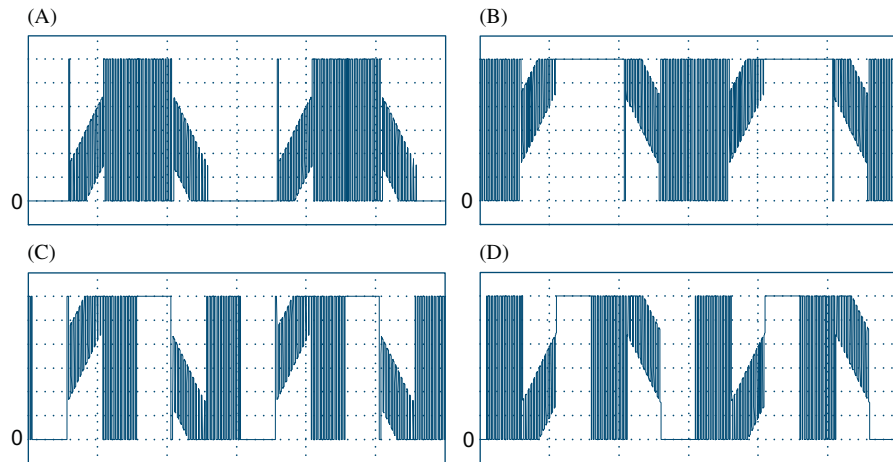
FIGURE 10.22

Back-EMFs according to unipolar PWM techniques: (A) upper switch PWM, (B) lower switch PWM, (C) on-going PWM, and (D) off-going PWM.

We have just now discussed the ZCPs of the back-EMF waveforms for a six-step drive in Fig. 10.20. However, BLDC motors are usually driven by using a PWM technique. In this case, PWM signals are superimposed on the back-EMF waveforms, as can be seen in Fig. 10.22. Thus, The ZPSs are obscured by the PWM signals. Several improved back-EMF sensing methods linked to PWM techniques, which require neither a virtual neutral voltage nor a great amount of filtering, have been introduced [14].

However, these back-EMF-based methods have intrinsic restrictions on low-speed operations where the back-EMF becomes insufficient. In addition, since there is no information on the back-EMF at start-up, an additional method for start-up is needed. Commonly, a sensorless BLDC motor is first started using initial rotor position detection method and brought up to a certain speed by an open-loop operation. When the motor reaches a speed where the back-EMF is sufficient to be sensed, the operation is transferred to the sensorless control.

REFERENCES

[1] G. Bauerlein, A brushless DC motor with solid-state commutation, IRE Natl. Conv. Rec. (1962) 184−190.
[2] T.M. Jahns, W.L. Soong, Pulsating torque minimization technique for permanent magnet AC motor drives—a review, IEEE Trans. Ind. Electron. 43 (2) (Apr. 1996) 321−330.
[3] P. Pillay, R. Krishnan, Modeling, simulation, and analysis of permanent-magnet motor drives, Part II. The brushless DC motor drive, IEEE Trans. Ind. Appl. 25 (2) (Mar./Apr. 1989) 274−279.
[4] R. Carlson, M. L-Mazenc, J. Fagundes, Analysis of torque ripple due to phase commutation in brushless DC machines, IEEE Trans. Ind. Appl. 28 (3) (1992) 441−450.
[5] C. Berendsen, G. Champenois, A. Bolopion, Commutation strategies for brushless DC motors: influence on instant torque, IEEE Trans. Power Electron. 8 (2) (1993) 231−236.
[6] K-W Lee, et al., Current control algorithm to reduce torque ripple in brushless DC motors, in: Conf. Rec. ICPE'98, vol. 1, Seoul, Korea, October 1998, pp. 380−385.
[7] J.H. Song, I. Choy, Commutation torque ripple reduction in brushless DC motor drives using a single DC current sensor, IEEE Trans. Power Electron. 19 (2) (Mar., 2004) 312−319.
[8] K.-J. Kwun, S.-H. Kim, A current control strategy for torque ripple reduction on brushless DC motor during commutation, Trans. Korean Inst. Power Electron. 9 (4) (Jun. 2002) 195−202.
[9] Z. Xiangjun. C. Boshi, The different influences of four PWM modes on the commutation torque ripples in sensorless brushless DC motors control system, in: Proc. the Fifth International Conference Electrical Machines and Systems, vol. 1, 2001, pp. 575−578.
[10] U. Vinatha, S. Pola, K.P. Vittal, A novel PWM scheme to eliminate the diode freewheeling in the inactive in BLDC motor, in: Conf. Rec. IEEE PESC'2004, pp. 2282−2286.
[11] K. Iizuka, et al., Microcomputer control for sensorless brushless motor, IEEE Trans. Ind. Appl. 27 (May/Jun., 1985) 595−601.
[12] P.P. Acarnley, J.F. Watson, Review of position-sensorless operation of brushless permanent-magnet machines, IEEE Trans. Ind. Electron. 53 (2) (Apr. 2006) 321−330.
[13] T. Kim, H.-W. Lee, M. Ehsani, Position sensorless brushless DC motor/generator drives: review and future trends, IET Electr. Power, Appl. 1 (4) (2007) 557−564.

[14] S. Ogasawara, H. Akagi, An approach to position sensorless drive for brushless DC motors, IEEE Trans. Ind. Appl. 27 (5) (Sep./Oct., 1991) 928−933.

[15] Y.-S. Lai, Y.-K. Linl, A unified approach to back-emf detection for brushless dc motor drives without current and hall sensors, in Conf. Rec. IEEE IECON 2006, pp. 1293−1298.